2009 International Symposium on Nonlinear Theory and its Applications
NOLTA'09, Sapporo, Japan, October 18-21, 2009

Signal detection inspired by mouse taste receptor cells

Katsumi Tateno†, Jun Igarashi‡, Kazuki Nakada†, Tsutomu Miki†, Yoshitaka Ohtubo†
and Kiyonori Yoshii†

†Department of Brain Science and Engineering, Kyushu Institute of Technology
Kitakyushu, 808-0196, Japan
‡(Present address;) RIKEN Computational Science Research Program, Integrated Simulation of Living Matter Group
Brain and Neural Systems Team
2-1 Hirosawa, Wako, Saitama, 351-0198, Japan
Email: tateno@brain.kyutech.ac.jp

Abstract—The present study shows a chemical sensor network model inspired by mouse taste receptor cells. The sensor array consisted of 10 Type II cell models and a pair of uncoupled Type III cell models. The Type II cell models elicit telegraph signals in response to the taste stimuli. The telegraph signals equally converge on the Type III cell models. The common telegraph signals increased the spiking frequency of the Type III cell models and facilitated spike synchronization. As a result, the taste stimulus is detected as the degree of synchronization and the spiking frequency of the output cells.

1. Introduction

Each taste bud consists of several tens of cells, which are classified into four types of cells (Type I to Type IV). The taste nerve has chemical synapses on only Type III cells. It means that Type III cell is the output cell of a taste bud. On the other hand, Type II cells have taste receptors for bitter, sweet, or umami. As Type II cells do not have synapses with the taste nerve, communications between Type II cells and Type III cells are necessary for taste signal processing. Nogami and his coworkers have shown possible signal transmissions between the taste bud cells [1]. That result suggests that the network in a single taste bud contributes to process taste information on tongues.

We have proposed a computational model of a chemical sensor array which consisted of the leaky integrate-and-fire (LIF) models and bursting models [2]. The LIF model and the bursting model corresponded to the Type II cell and the Type III cell respectively. The chemical stimulus is detected as the degree of synchronization of bursts. However, that Type II cell model was over-simplified. Further, the Type III cell is not a bursting cell.

The sodium channel of the mouse taste receptor cells shows slow recovery from inactivation. The slow recovery from sodium inactivation accounts long interpulse intervals of the taste receptor cells. Further, even when relatively strong current is injected the taste receptor cells exhibit a single action potential. The membrane potential remains stable after the overshoot. On the other hand, the outward current of the Type III cells is the delayed rectifier potassium current, while the outward current of the Type II cells is TEA-insensitive current [3]. Differences in the outward currents potentially alter spike patterns of the taste receptor cells. Such spiking properties caused by the ion channels contribute to the chemical signal detection in the present network model. The chemical signal is detected as the degree of synchronization and the spiking frequency of the output cells.

2. Methods

The present chemical sensor array consisted of 10 Type II cell models and 2 Type III cell models. No connection existed among the Type II cell models. Output of the Type II cell models equally converged on the Type III cell models.

2.1. Type II cell model

We used a transient sodium model (I_{nat} model) [4] as the Type II cell. The I_{nat} model consisted of the transient sodium current and the leak current.

$$C_m \frac{dv_i}{dt} = -\bar{g}_{\mathrm{Na}} \cdot m_{\infty,i}^3 \cdot h_i \cdot (v_i - e_{\mathrm{Na}}) - g_l \cdot (v_i - e_l) + i_{\mathrm{dc}} + \xi_i(t) \quad (1)$$

$$\frac{dh_i}{dt} = \frac{h_{\infty,i}(v_i) - h_i}{\tau_h(v_i)} \quad (2)$$

Here, i = 1, 2, ..., 10. The parameters were fixed at C_m = 1 μF/cm^2, e_l = -60 mV, e_{Na} = 60 mV, and $\bar{g}_{\mathrm{Na}}$ = 15 mS/cm^2. The leak conductance g_l was 0.6 ~ 1 mS/cm^2. $\xi_i(t)$ is the Gaussian noise. $< \xi_i(t)\xi_i(t') >= \sigma_{\mathrm{nat}}^2 \delta(t - t')$. σ_{nat} = 2 mV·ms$^{-1/2}$ unless otherwise specified.

The rate function of the sodium current is below:

$$m_\infty(v_i) = \frac{1}{1 + \exp((-40 - v_i)/9)} \quad (3)$$

$$h_\infty(v_i) = \frac{1}{1 + \exp((62 + v_i)/7)} \quad (4)$$

$$\tau_h(v_i) = 1.2 + C_{\mathrm{amp}} * \exp(-\frac{(-67 - v_i)^2}{400}) \quad (5)$$

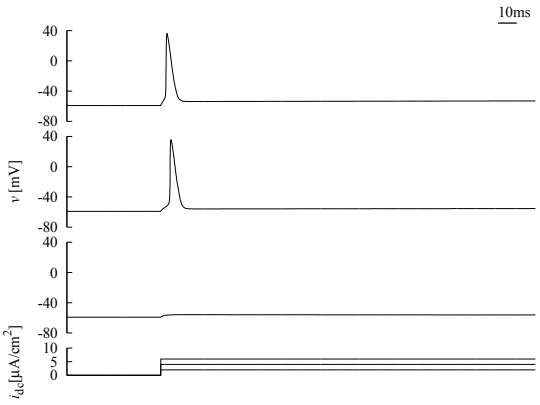

Figure 1: Step currents elicited a single action potential in the I_{nat} model. Stable membrane potential followed the spike discharge. g_l = 1 mS/cm^2. Top: i_{dc} = 6 μA/cm^2; Middle: i_{dc} = 4 μA/cm^2; Bottom: i_{dc} = 2 μA/cm^2. σ_{nat} = 0 mV·ms$^{-1/2}$.

The inactivation variable h_i of the sodium current has a voltage-dependent time constant. The mouse taste receptor cells take ∼1 s for recovery from inactivation [5]. Here, C_{amp} = 740 ms, which is 100 times larger than a typical value reported by Izhikevich [4].

The I_{nat} model exhibits class 3 excitability. The step current elicits a spike, but the membrane potential remains stable after the overshoot (Fig. 1).

2.2. Type III cell model

The Type III cell model is a one-dimensional model described below:

$$\varepsilon \frac{d\psi_j(t)}{dt} = 1 - \epsilon \sin \psi_j(t) + s(t) + \zeta_j(t) \quad (j = 1, 2) \quad (6)$$

where ε = 20 ms and ϵ = 1.1. The cells were identical. The unit of ψ is arbitrary. $s(t)$ is the telegraph signal generated by the I_{nat} models. $s(t)$ jumps between 0 and 1. In Sec 3.1, we used the random telegraph noise for $s(t)$. In that case, $s(t)$ is stochastically jumps between 0 and 1. $\zeta_i(t)$ is the Gaussian noise. $< \zeta_i(t)\zeta_i(t') >= \sigma_t^2 \delta(t - t')$. σ_t = 0.01 ms$^{-1/2}$.

The Type III cell model has two fixed points; one is stable and the other is unstable. The unstable fixed point is the threshold of the action potential. If ψ is beyond the unstable fixed point, ψ increases. When $\psi = 2\pi$, a spike occurs and ψ is set to 0.

2.3. Computer simulations

Prior to simulations of the complete network model, we separately stimulated each part. First, we simultaneously stimulated a pair of the Type III cell models by the random telegraph noise. The random telegraph noise was equally given to the Type III cell models. The degree of synchronization of spikes was assessed. The interpulse intervals of the random telegraph noise were drawn from the exponential distribution. The random telegraph noise stochastically jumps between 0 and 1. The time constant of each state was separately determined. The escape rate from 1 to 0 is k_{up} (= 0.2 ms^{-1}). It means that the mean duration of the upper state was 5 ms. The escape rate from 0 to 1 is k_{low} (= 0.001 ∼ 1 ms^{-1}). In short, the mean duration of the lower state (= T) was 1 ∼ 1000 ms.

The degree of synchronization of spikes in the pair of the Type III cell models was quantified by the equation followed:

$$\gamma^2 =< \sin \Delta\phi >^2 + < \cos \Delta\phi >^2 \quad (7)$$

where $\Delta\phi$ is the phase difference between the cells. $< \cdot >$ means the average in time. Simulations was performed for 100 s.

Second, interpulse intervals generated by 10 I_{nat} models were obtained. The I_{nat} models were identical. The I_{nat} models randomly fire due to the Gaussian noise. We collected interpulse intervals of all I_{nat} models for 20 s (or 40 s when g_l = 1 mS/cm^2) and made density histograms. The interpulse intervals are the duration of the lower state ($v_i < -40$ mV). The mean value and the standard deviation of the interpulse intervals were calculated. The coefficient of variation, CV = SD/mean, was also calculated. We obtained the density histograms of the interpulse intervals at each g_l (= 0.6 ∼ 1 mS/cm^2).

Finally, the I_{nat} models were connected to the Type III cell models. We assumed that taste substances alter g_l of the I_{nat} models (g_l = 0.6∼1 mS/cm^2). The I_{nat} models generate the random telegraph signals, and the Type III cell models output spikes to the taste nerves. During $v_i > -40$ mV, $s(t) = 1$. Otherwise, $s(t) = 0$. The telegraph signals equally converged on the Type III cell models. The degree of synchronization of spikes in the pair of the Type III cell models was assessed. The spiking frequency of the Type III cell model #1 was counted. The I_{nat} models were identical unless otherwise stated. The computations were repeated 10 times at each g_l. The computational time was 40 s. The numerical integration was performed by the forward Euler scheme. The time step was 0.001 ms.

3. Results

3.1. Synchronization of the Type III cell models induced by the random telegraph noise

A pair of uncoupled identical Type III cell models was synchronized by the common random telegraph noise. When T of the random telegraph noise was in the range between 10 ms and 100 ms, γ was high and the spiking frequency increased (Fig. 2). At small T, the spiking frequency was high, but low γ values. As $s(t)$ frequently jumps to 1, ψ hardly remains the stable fixed point. Such fluctuations lowered the degree of synchronization of spikes.

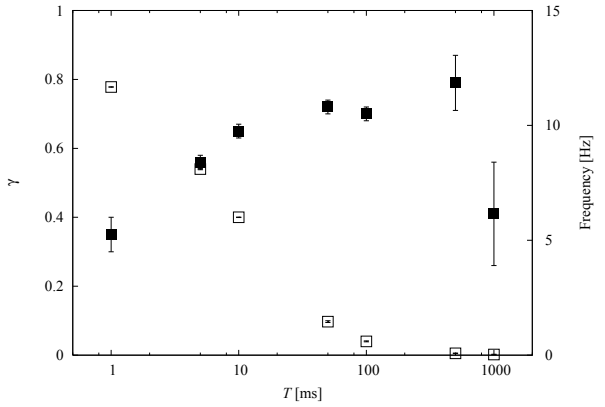

Figure 2: Spike synchronization induced by the random telegraph noise in a pair of the Type III cell models. In the range between 10 ms and 500 ms of T, the synchronization index γ (■) was high. The spiking frequency (□) exponentially decreased with an increase in T. $\sigma_t = 0.01$ ms$^{-1/2}$.

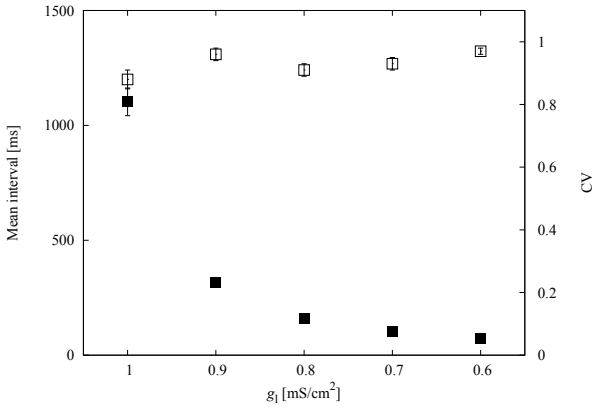

Figure 3: Interpulse intervals of the telegraph signals generated by the array of the I_{nat} models were exponential-like distributions. ■: Mean interval. □: Coefficient of variation (CV). $\sigma_{\mathrm{nat}} = 2$ mV·ms$^{-1/2}$.

At $T \geq 500$ ms, the spiking frequency was almost 0, but γ was high with large error bars. In most simulations γ was low, but, in a few cases, γ was nearly 1. This is because two or three spikes luckily occurred at both Type III cell models at the same time in the simulations.

3.2. Telegraph signals generated by the array of the I_{nat} models

Due to the Gaussian noise, a single I_{nat} model showed a gamma-like or Gaussian-like interval distributions. The interval distributions depended on the leak conductance g_l. When g_l got smaller, density histograms of the interpulse intervals were the Gaussian-like distribution.

The array of 10 I_{nat} models exhibited the exponential-like interval distributions. The mean intervals of the interval distributions exponentially decreased with a decrease in g_l (Fig. 3). CVs were nearly 1 in the range $g_l < 0.9$ mS/cm^2. When g_l was 0.6 mS/cm^2 or 0.7 mS/cm^2, the mean intervals were below 100 ms. At $g_l = 1$ mS/cm^2, a few pulses were elicited. Those results indicate that the array of the I_{nat} models potentially induces spike synchronization in the Type III cell models in the range between 0.6 and 0.7 mS/cm^2 of g_l.

3.3. Synchronization of the Type III cell models in the sensor network model

The I_{nat} models randomly fired due to the Gaussian noise ($g_l = 0.6$ mS/cm^2, Top trace in Fig. 4a). Spikes of the 10 I_{nat} models were converted to the telegraph signals (Second trace in Fig. 4a). The common telegraph signal induced synchronization of spikes in the Type III cell models (Bottom two traces in Fig. 4a). γ and the spiking frequency were summarized in Fig. 4b. At small g_l, γ and the spiking frequency were high. As a result, the taste stimulus is detected as synchronized spikes with high spiking frequency.

We further used non-identical I_{nat} models. g_l were randomly determined. The standard deviation of g_l was 0.1 × the mean value (= 0.6 ~ 1 mS/cm^2). The telegraph signals were generated by the array of 10 non-identical I_{nat} models. Those common telegraph signals induced synchronization of spikes in the Type III cell models (data not shown). γ values and the spiking frequency increased with a decrease in g_l.

4. Discussion

Synchronization of uncoupled oscillators induced by the Gaussian noise is known as noise-induced synchronization. Random telegraph noise also induces synchronization of oscillators [7]. The common random telegraph noise induced synchronization of spikes in a pair of uncoupled Type III cell models in the present study. The present Type III cell model is not in the oscillatory mode, but excitable. As the Type III cell models were identical, both ψs existed around the fixed point. The common telegraph signals depolarize both the Type III cell models. If such depolarizations are strong, the Type III cell models simultaneously fire. In the present study, the mean duration of depolarization, actually the duration of action potentials of the I_{nat} models, was mostly ~5 ms. As depolarization by the common telegraph signal is long enough to elicit spikes, spike synchronization is less dependent on the duration of the lower state of the common random telegraph signals. Frequent depolarizations rather disturb synchronization of output spikes. If the array of the I_{nat} models pauses excitations for 10 ~100 ms, spike synchronization is facilitated in the Type III cell models.

Mouse taste receptor cells are not fast-spiking cells [8].

a

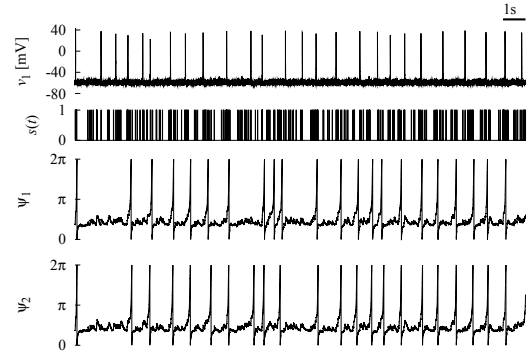

b

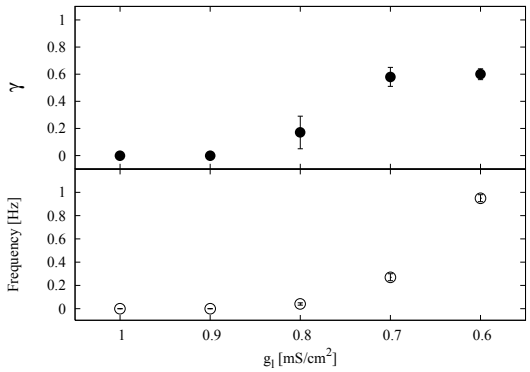

Figure 4: Spike synchronization in the Type III cell models in the sensor network model. a. Telegraph signals $s(t)$ generated by the array of the I_{nat} models induced synchronization of spikes in the Type III cell models. $g_l = 0.6$ mS/cm^2. Data were plotted at every 100 integration steps. b. Synchronization index γ (•) and the spiking frequency (○) of the Type III cell models. γ and the spiking frequency increased with a decrease in g_l. $\sigma_{\mathrm{nat}} = 2$ mV·ms$^{-1/2}$. $\sigma_{\mathrm{t}} = 0.01$ ms$^{-1/2}$

The step current elicits a single spike or a few spikes. Further, the slow recovery from inactivation of the sodium channel causes long pauses of interpulse intervals of the taste receptor cells. The present I_{nat} models have the slow recovery from sodium inactivation and exhibit class 3 excitability. Under the Gaussian noise, the interpulse intervals of the single I_{nat} model were gamma-like distributions with long mean intervals. As a result, the array of the I_{nat} models exhibits adequate long period of inter-train pauses and stochastic alternations between 0 and 1 on the common telegraph signals.

Taste stimuli elicit not only depolarization of the membrane potential in the mouse taste receptor cells, but also hyperpolarization. Ohtubo and his coworkers have reported that taste stimuli caused membrane depolarization or hyperpolarization in the mouse taste receptor cells [6]. Complex responses of the mouse taste receptor cells might contribute to signal processing in the taste buds. If the taste stimuli depress some of the I_{nat} models in the sensor array, the frequency of the telegraph signal reduces but its patterns can be still random. The mouse taste bud-like complex responses can induce spike synchronization in the output cells.

Acknowledgments

This work was supported by a COE program (center #J19) granted to Kyushu Institute of Technology by MEXT of Japan.

References

[1] W. Nogami, R. Hayato, K. Eguchi, and K. Yoshii, "Propagation of Ca^{2+} responses among taste bud cells," International Congress Series, vol.1301, pp.258-261, 2007.

[2] K. Tateno, K. Yoshii, Y. Ohtubo, and T. Miki, "A network model toward a taste bud inspired sensor," International Congress Series, vol.1301, pp.52-55, 2007.

[3] K. Kimura, Y. Ohtubo, T. Kumazawa, and K. Yoshii, "Electrophysiological identification of mouse taste bud cells," International Congress Series, vol.1301, pp.254-257, 2007.

[4] E. M. Izhikevich, "Dynamical Systems in Neuroscience," MIT Press, 2007.

[5] Y. Ohtubo, Y. Hashiba, K. Kimura, T. Kumazawa, and K. Yoshii, "Voltage-gated Na^+ currents of each cell type in mouse taste buds", Abstract of ECRO2008, p. 83, 2008.

[6] Y. Ohtubo, T. Suemitsu, S. Shiobara, T. Matsumoto, T. Kumazawa, and K. Yoshii, "Optical recordings of taste responses from fungiform papillae of mouse in situ," Journal of physiology, vol.530, pp.287-293, 2001.

[7] K. Nagai, H. Nakao, and Y. Tsubo, "Synchrony of neural oscillators induced by random telegraphic currents," Physical Review E, vol.71, 036217, 2005.

[8] T. Noguchi, Y. Ikeda, M. Miyajima, and K. Yoshii, "Voltage-gated channels involved in taste responses and characterizing taste bud cells in mouse soft palates," Brain Research, vol.982, pp.241-259, 2003.